β-Cell Hyperplasia Induced by Hepatic Insulin Resistance

Role of a Liver-Pancreas Endocrine Axis Through Insulin Receptor A Isoform

Oscar Escribano,[1,2] Carlos Guillén,[1,2] Carmen Nevado,[1,2] Almudena Gómez-Hernández,[1,2] C. Ronald Kahn,[3] and Manuel Benito[1,2]

OBJECTIVE—Type 2 diabetes results from a combination of insulin resistance and impaired insulin secretion. To directly address the effects of hepatic insulin resistance in adult animals, we developed an inducible liver-specific insulin receptor knockout mouse (iLIRKO).

RESEARCH DESIGN AND METHODS—Using this approach, we were able to induce variable insulin receptor (IR) deficiency in a tissue-specific manner (liver mosaicism).

RESULTS—iLIRKO mice presented progressive hepatic and extrahepatic insulin resistance without liver dysfunction. Initially, iLIRKO mice displayed hyperinsulinemia and increased β-cell mass, the extent of which was proportional to the deletion of hepatic IR. Our studies of iLIRKO suggest a cause-and-effect relationship between progressive insulin resistance and the fold increase of plasma insulin levels and β-cell mass. Ultimately, the β-cells failed to secrete sufficient insulin, leading to uncontrolled diabetes. We observed that hepatic IGF-1 expression was enhanced in iLIRKO mice, resulting in an increase of circulating IGF-1. Concurrently, the IR-A isoform was upregulated in hyperplastic β-cells of iLIRKO mice and IGF-1–induced proliferation was higher than in the controls. In mouse β-cell lines, IR-A, but not IR-B, conferred a proliferative capacity in response to insulin or IGF-1, providing a potential explanation for the β-cell hyperplasia induced by liver insulin resistance in iLIRKO mice.

CONCLUSIONS—Our studies of iLIRKO mice suggest a liver-pancreas endocrine axis in which IGF-1 functions as a liver-derived growth factor to promote compensatory pancreatic islet hyperplasia through IR-A. *Diabetes* **58:820–828, 2009**

Type 2 diabetes results from a combination of insulin resistance and impaired insulin secretion. Although there is some debate about the primary defect underlying type 2 diabetes, insulin resistance is the most relevant pathophysiological feature of the pre-diabetes state (1,2). Rodent studies have shown that insulin insensitivity in both classic and nonclassic insulin target tissues can play a role in the control of glucose homeostasis (3). Insulin resistance also produces a compensatory increase in insulin secretion generating hyperinsulinemia, and ultimately, it is the failure of the β-cell that causes fasting hyperglycemia and development of type 2 diabetes (1). Several mouse models have been developed to study the contributions of insulin resistance in various tissues to the overall regulation of glucose homeostasis (4). Although total whole-body insulin resistance produced by complete deletion of the insulin receptor (IR) does not produce any major effect on mouse development, these mice die 1 week after birth from severe ketosis (5,6). Combined restoration of IR function in brain, liver, and pancreatic β-cells rescues IR knockout mice from neonatal death, prevents diabetes in a majority of animals, and normalizes adipose tissue content, lifespan, and reproductive function. In contrast, mice with IR expression limited to brain or liver and pancreatic β-cells are rescued from neonatal death but develop lipoatrophic diabetes and die prematurely (7).

Based on studies using tissue-specific conditional knockout of IR, liver, brain, and β-cells represent the key sites of insulin resistance in the development of type 2 diabetes (8–10). The liver-specific IR knockout (LIRKO) revealed that insulin resistance in liver is the most important for development of impaired glucose tolerance and fasting hyperglycemia. In addition, these mice also developed marked β-cell hyperplasia, hyperinsulinemia, and decreased insulin clearance (8). With aging, however, the diabetes in these animals was corrected, suggesting some form of compensatory mechanism possibly linked to the very early onset of insulin resistance in these mice that limited understanding of the full impact of hepatic insulin resistance in the pathogenesis of type 2 diabetes. Moreover, these mice developed liver damage related to appearance of hyperplastic nodules that might have altered glucose production by the liver, leading to regression of the diabetic state with aging (8). To better address the role of adult hepatic insulin resistance in the pathogenesis of type 2 diabetes, we developed an inducible model for generating liver IR deficiency (iLIRKO) in young, weaned mice.

RESEARCH DESIGN AND METHODS

IR[(loxP/loxP)] C57Bl/6 mice were created by homologous recombination using an IR gene targeting vector with lox P sites flanking exon four as previously described (11). Transgenic mice expressing a *Cre* recombinase transgene under the control of the Mx1 promoter/enhancer were purchased from Jackson Laboratory (Bar Harbor, ME). The IR[(loxP/loxP)] mice were crossed with Mx-Cre mice to obtain iLIRKO mice. After weaning, iLIRKO mice were injected intraperitoneally with poly-inositic-poly-cytidilic acid (500 μg/injection) to induce the interferon-α response and the consequent Mx1 promoter

activation as described previously with minor modifications (12). Animals were housed in virus-free facilities on a 12-h light-dark cycle (on at 0700 h, off at 1900 h) and were fed with a standard rodent chow ad libitum. All animal experimentation described in this article was conducted in accordance with accepted standards of humane animal use as approved by the corresponding institutional committee.

Genotyping of the IR^(loxP/loxP) transgenic mice. IR^(loxP/loxP) transgenic mice were genotyped by PCR. Tail DNA (100–200 ng) was amplified 30 cycles (40 s, 94°C; 40 s, 60°C; and 1 min, 75°C) by a thermal cycler. Two primers flanking the *loxP* site behind exon four of the IR were used: the forward primer (5′-GATGTGCACCCCATGTCTG-3′) and the reverse primer (5′-CT-GAATAGCTGAGACCACAG-3′). A 320-bp band was obtained for the floxed allele or a 280-bp band for the wild-type allele.

Genotyping of the Mx1-Cre transgenic mice. Mx1-Cre transgenic mice were genotyped by PCR. Tail DNA (100–200 ng) was amplified 35 cycles (1 min, 94°C; 1 min, 60°C; and 1 min, 72°C) on a thermal cycler. To amplify the Mx1-Cre transgene (PCR product, 269 bp), primers SF-4 (5′-GCATAACCAGT-GAAACAGCATTGCTG-3′) and 69R (5′-GGACATGTTCAGGGATCGCCAG-GCG-3′) were used.

Western blot analysis. Tissues were homogenized as described (11). Western blot analyses of insulin signaling proteins were performed on liver, muscle, brown adipose tissue, and brain homogenates as previously described (13). The antibodies used were anti-IRβ (Ab-4) from Oncogene (San Diego, CA), anti-PEPCK antibody provided by D.K. Granner (Vanderbilt University, Nashville, TN), anti-glucokinase antibody (a gift of S. Lenzen, Hannover Medical School, Hannover, Germany), anti–fatty acid synthase antibody (purchased from BD Transduction Laboratories, San Diego, CA), and anti–β-actin antibody (Sigma-Aldrich, St. Louis, MO). Anti–IGF-1 antibody was purchased from Upstate Biotechnology (Lake Placid, NY). Anti–phospho-p70-S6-kinase (Thr 421/Ser 424), anti–phospho-p44/p42-MAPK (Thr202/Tyr204), anti–phospho-Akt (Ser 473) antibodies were purchased from Cell Signaling (Beverly, MA). For in vivo insulin signaling studies, mice were injected with 1 unit/kg body wt of human insulin (Novo Nordisk) into the peritoneal cavity. After 10 min, tissues were removed and immediately frozen in liquid nitrogen. Triplicate blots of samples from five individuals of each genotype were used. Densitometric analysis was performed using a GS-710 Imaging Densitometer, and signals were quantified using Quantity One software (Bio-Rad Laboratories, Hercules, CA).

Analytical procedures. Insulin levels in serum were measured by RIA using mouse insulin as a standard (Linco Research, St. Charles, MO). Radioimmunoassay using mouse IGF-1 as a standard (Diagnostic Systems Laboratories, Webster, TX) measured IGF-1 levels in serum. Glucose tolerance and insulin tolerance tests were performed as previously described (14).

Histological analysis. The immunohistochemical analysis of pancreata was performed as described (14). β-Cell mass was evaluated by point-counting morphometry (15,16). Relative volumes were calculated for β-cells, non–β-cells, and exocrine tissue. Contaminating tissue (including adipose, lymph nodes, and intestines) was recorded to correct for the pancreatic weight. The β-cell mass was then calculated by multiplying the relative β-cell volume by the corrected pancreatic weight. Staining of liver sections with hematoxylin/eosin, periodic acid Schiff, and Masson reagents was performed using standard techniques.

Real-time quantitative PCR for insulin receptor isoforms. The pancreatic islets were isolated from 6-month-old control and iLIRKO mice as previously described (10). Insulin receptor isoforms expression in isolated islets was analyzed by real-time quantitative PCR using Taqman probes (MGB "Assay on Demand" probes; Applied Biosystems) following the manufacturer's instructions. The comparative threshold cycle (Ct) method was used to calculate the relative expression. For quantification of gene expression, the target genes values were normalized to the expression of the endogenous reference (18S). Thus, the amount of target, normalized to 18S and relative to the control, is given by $2^{-\Delta\Delta Ct}$ [$\Delta Ct = Ct$ (target gene) − Ct (18S); $\Delta\Delta Ct = \Delta Ct$ for any sample − ΔCt for the control].

Reconstitution of IRKO immortalized β-cells with IR-A or -B isoforms by retroviral infection. IRKO β-cells were generated in our laboratory as previously described (17). From these cells we reconstituted and characterized the expression of the IR-A isoform (Rec A) and IR-B isoform (Rec B) generating new cell lines as previously described (18).

Measurement of glucose uptake in β-cells. Cells were cultured to 80% confluence in 10% FBS-DMEM and then serum and glucose starved for 4–6 h. After that, 10 nmol/l insulin or 10 nmol/l IGF-1 were added to the wells for 30 min. Glucose uptake was measured by incubating cells with 2-deoxy-D-[1-³H]-glucose for the last 10 min in triplicate dishes from six independent experiments as previously described (19).

Cell viability assays. Cells were plated in 12-multiwell plates and cultured in 10% FBS-DMEM until 40–50% of confluence was reached. Cells were deprived of serum for a minimum of 4 h and then treated with insulin (10 nmol/l), IGF-1

(10 nmol/l), or both for 24 h. Subsequently, the cells were washed with PBS and stained with violet crystal as described (17).

Proliferation studies in isolated pancreatic islets and cultured β-cells. DNA synthesis in isolated islets was estimated by determining BrdU incorporation using the Cell Proliferation ELISA kit (Roche Diagnostics, Mannheim, Germany). In cultured β-cells, the DNA synthesis was estimated by [³H] thymidine incorporation into trichloroacetic acid–precipitable material as previously described (20).

All values are expressed as means ± SEM. Data were compared by ANOVA with the Bonferroni post-test or the Student's *t* test. The level of significance was set at $P < 0.05$.

RESULTS

Progressive liver-specific insulin receptor deletion without liver dysfunction. To create an inducible liver-specific deletion of the IR, IR^(loxP/loxP) mice (11) were bred with transgenic mice expressing a *Cre* recombinase transgene under the control of the Mx1 promoter/enhancer. Finally, we obtained mice that all carried two floxed IR alleles and were heterozygous for the Mx1-Cre transgene. Thus, these mice constituted the iLIRKO mouse strain. Given that the deletion of IR varied from ~50–100%, mice were divided into three groups: ones with ~50% of the normal receptor expression, a second group with mice bearing ~25% of normal IR, and a third group containing mice with virtually no remaining IR. Ablation of IR was tissue specific because none of the other insulin target tissues was affected (results not shown). An important feature of the phenotype produced by fetal IR deletion (LIRKO) was the appearance of liver dysfunction and histological changes. However, hematoxylin-eosin staining in liver sections revealed no dysplastic or hyperplastic nodules in 6- and 12-month-old iLIRKO mice as compared with their respective controls. In addition, Masson staining showed no increase in collagen infiltration or fibrosis in iLIRKO mice (Fig. 1, *upper panels*). Regarding enzymes of hepatic glucose metabolism, postnatal deletion of IR caused a reduction of glucokinase protein expression and a dramatic loss of glycogen liver content in iLIRKO mice consistent with previous observations in the LIRKO model (8). However, the expression of phosphoenol pyruvate carboxykinase or fatty acid synthase genes in 6-month-old mice was unchanged in iLIRKO mice as compared with controls (Fig. 1, *lower panels*).

Progressive insulin resistance and glucose intolerance in iLIRKO. In LIRKO mice, insulin signaling in vivo is selectively impaired in liver because these mice display normal insulin sensitivity in skeletal muscle (8). At 6 months of age, iLIRKO mice presented defects in insulin signaling, which were proportional to their loss of IR expression. Thus, in the group with 50% reduction in IR expression, there was a marked decrease in Akt, extracellular signal–related kinases (ERKs), and p70S6-kinase activation, whereas in the group with complete IR deletion, insulin was unable to activate these signaling pathways (Fig. 2). Interestingly, although our deletion strategy did not alter the levels of IR expression in other tissues (results not shown), we observed progressive impairment of insulin signaling in some peripheral tissues. Thus, in iLIRKO mice, there was a graded impairment of insulin-stimulated Akt and ERKs signaling in brain, skeletal muscle, or interscapular brown adipose tissue, the degree of which correlated with the severity of IR deletion in the liver (Fig. 2). Similarly, p70S6-kinase signaling was impaired in response to insulin in these tissues and was dependent as well on hepatic IR expression. Insulin signaling in both liver and these extrahepatic tissues was
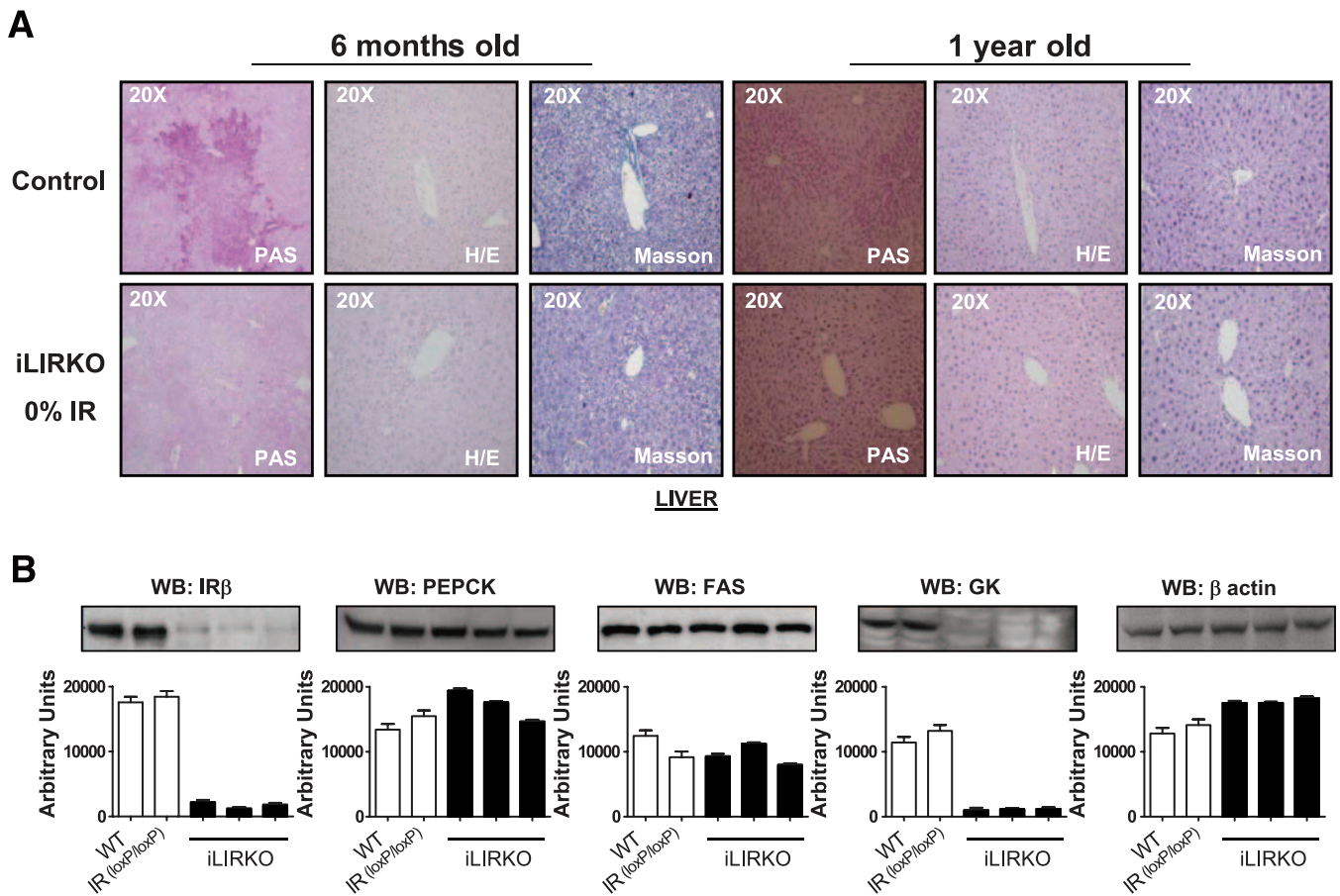
FIG. 1. Liver histology and metabolic gene expression in inducible liver-specific insulin receptor knockout (iLIRKO) mice. *A*: Periodic acid Schiff, hematoxylin-eosin (H/E), and Masson staining of liver sections from fed 6- and 12-month-old male control (*upper panel*) and iLIRKO (*lower panel*) mice. The images are representative of four independent experiments. Magnifications 20×. *B*: Protein extracts of liver from 6-month-old Wt (wild type), IR$^{(loxP/loxP)}$, and iLIRKO mice were analyzed by Western blot (WB) with anti-IR β-chain, PEPCK, FAS (fatty acid synthase), GK, and β-actin antibodies as indicated in each panel. The blots are representative of five independent experiments. The corresponding autoradiograms were quantitated by scanning densitometry and are expressed as mean ± SEM. (A high-quality digital representation of this figure is available in the online issue.)

markedly impaired in 1-year-old iLIRKO mice (results not shown). Our results indicate that the iLIRKO mouse develops primary insulin resistance in the liver, and this is associated with secondary insulin resistance in peripheral tissues, which persists throughout the life of the animal. In conventional LIRKO mice, IR deletion induced severe insulin resistance, which caused glucose intolerance at 2 months of age, but this diabetic phenotype was completely reversed by 6 months of age when these mice presented normal glucose tolerance (8). In contrast, our strategy of deleting the IR after weaning induced progressive insulin resistance in iLIRKO mice from 2 to 6 months old and this persisted at 1 year of age (Fig. 3, *upper panels*). More importantly, the mice without liver IR displayed progressive glucose intolerance and even developed fasting hyperglycemia at 1 year of age (Fig. 3, *lower panels*).

Progressive β-cell hyperplasia and failure of insulin secretion with aging. Previously, it was shown that constitutive LIRKO mice developed severe hyperinsulinemia and β-cell hyperplasia by 2 months of age, and this fasting hyperinsulinemia remained unchanged although the glucose intolerance reverted with aging (8). In the present study, iLIRKO presented progressive β-cell hyperplasia as compared with controls. More importantly, the level of hyperplasia was correlated to the level of IR expression in the liver (Fig. 4*B*). The iLIRKO mice also

developed progressive hyperinsulinemia as compared with controls, and this also correlated with the extent of IR deletion in the liver (Fig. 4*B*). This β-cell expansion persisted throughout life as shown in Fig. 4*D*. In parallel, plasma insulin increased by 2.5-fold in 1-year-old mice as compared with their controls (Fig. 4*D*); however, this increase was much lower than at 6 months of age (threefold, Fig. 4*D*), suggesting a failure of insulin secretion with aging. Additionally, insulin content in pancreas slides of 6-month-old and 1-year-old iLIRKO mice was quantified. The data revealed a 25% increase in the insulin content ($P < 0.0001$) in 1-year-old as compared with 6-month-old iLIRKO mice (results not shown).

Progressive hepatic expression and plasma concentration of IGF-1 in iLIRKO mice. Previous studies have suggested the presence of a circulating islet growth factor in insulin-resistant states independent of glucose and obesity (21). To address this important issue, we performed Western blot analysis of iLIRKO liver samples using anti–IGF-1 antibodies. We observed increases of IGF-1 expression that depended inversely on the level of IR expression in the liver (Fig. 4*A*). In parallel, IGFBP1 and IGFBP3 were also upregulated in iLIRKO mice depending on the extent of IR deletion in liver. These data were confirmed in 1-year-old mice (Fig. 4*C*). Interestingly, iLIRKO mice, which expressed no liver IR,

6 months old

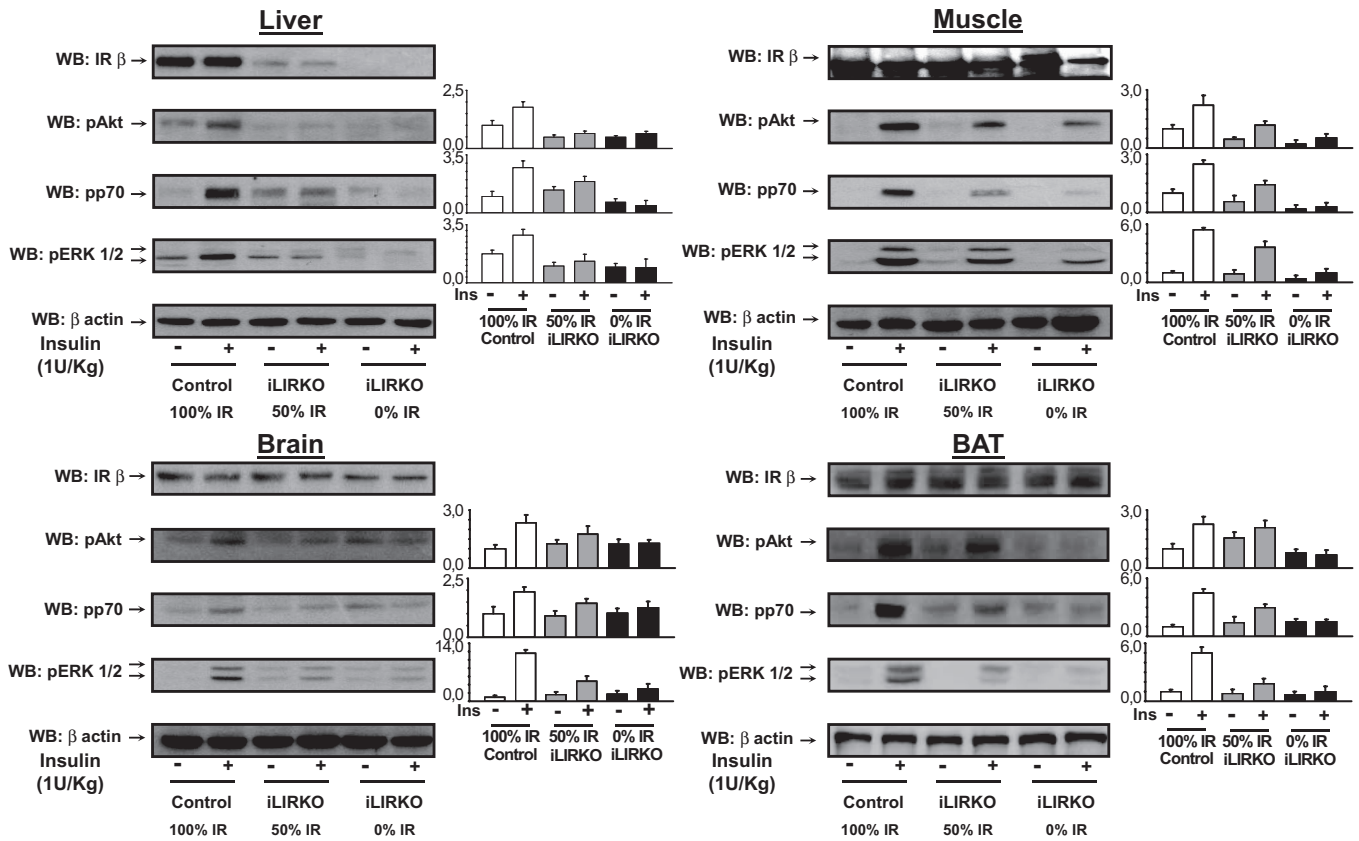**FIG. 2. Inducible liver-specific insulin receptor knockout (iLIRKO) shows insulin resistance in the liver and extrahepatic tissues. In vivo insulin signaling studies were performed in 6-month-old control and iLIRKO mice. Mice of both experimental groups were injected with 1 unit/kg body wt of human insulin (Novo Nordisk) into the peritoneal cavity. After 10 min of treatment, liver, muscle, BAT (brown adipose tissue), and brain were removed. Protein extracts of these tissues were analyzed by Western blot (WB) with anti-IR β-chain, phospho-Akt, phospho-p70, phospho-ERK1/2, and β-actin antibodies. The results are representative of four independent experiments. Histograms summarize the densitometric analysis of the corresponding Western blots.**

had significantly increased levels of plasma IGF-1 at 6 months and 1 year of age as compared with controls (Fig. 4*B* and *D*, respectively).

Increase of IR-A isoform in pancreatic islets: β-cell lines expressing IR-A, but not IR-B, induce proliferation in response to insulin or IGF-1. The IR expression in pancreatic islets, as estimated by real-time PCR, significantly increased in iLIRKO mice as compared with controls (Fig. 5*A*). More importantly, the percentage of IR-A isoform (IR-A) expressed in pancreatic islets dramatically increased in iLIRKO mice as compared with controls (Fig. 5*A*). To assess whether the balance of IR-A versus IR-B might alter the proliferation rate of islets, we analyzed BrdU incorporation in response to either 10 nmol/l insulin or 10 nmol/l IGF-1 in pancreatic islets of 6-month-old mice. The results demonstrated that IGF-1–induced proliferation was significantly higher in pancreatic islets from iLIRKO mice than in the controls (Fig. 5*B*). Previous reports suggest that IR-A was twofold more sensitive than IR-B in mediating glycogen synthesis and mitogenesis (22). To further explore these possibilities in mouse β-cells, we generated β-cell lines bearing IR (IRLoxP), lacking IR (IRKO), expressing exclusively IR-A (Rec A), or expressing exclusively IR-B (Rec B) (Fig. 5*C*). Cell lines expressing IR responded to 10 nmol/l insulin in contrast to cells lacking IR as determined by Western blot analysis of IR phosphorylation (Fig. 5*D*). Additionally, the four cell lines

responded to 10 nmol/l IGF-1 as confirmed by IGF-1R phosphorylation (Fig. 5*D*). The lack of IR significantly decreased basal glucose uptake in β-cells. Reconstitution with IR-A, but not with IR-B, restored basal glucose uptake to levels higher than those observed in control cells (Fig. 5*E*). Although either insulin or IGF-1 enhanced cell viability in control cells, only IGF-1 induced cell viability in β-cells lacking IR. Rec A cells but not Rec B increased cell viability in response to either insulin or IGF-1 (Fig. 5*F*). When we assessed proliferation by thymidine incorporation, both insulin and IGF-1 increased proliferation in control β-cells, whereas cell lines lacking IR did not respond to IGF-1. Finally, insulin and IGF-1 promoted proliferation in Rec A β-cells but not in Rec B lines (Fig. 5*G*).

DISCUSSION

Insulin promotes both metabolism and growth in the liver. Constitutive ablation of IR in liver causes severe metabolic changes and a reduction of liver size by ~50% (8). Likewise, mice in which there is variable IR deletion (cellular mosaicism) exhibit different degrees of growth retardation and metabolic abnormality depending on the extent of IR deletion. IR ablation in ~80% of cells causes extreme growth retardation and lipoatrophy with β-cell hyperplasia, whereas IR ablation in 98% of cells, although resulting
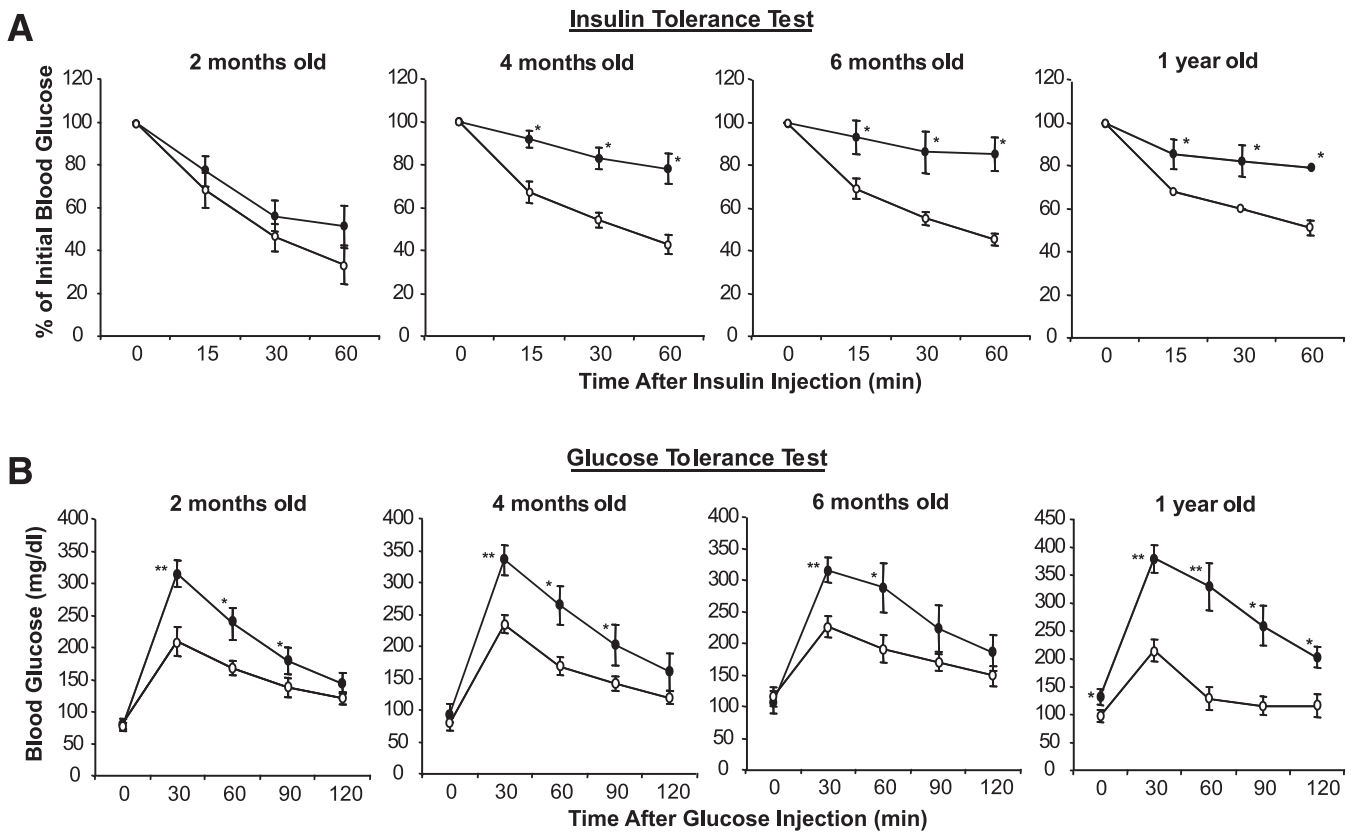
FIG. 3. Progressive insulin resistance and glucose intolerance in inducible liver-specific insulin receptor knockout (iLIRKO) mice. *A*: Insulin tolerance tests were performed on 2-, 4-, 6-, and 12-month-old male control (○) and iLIRKO (●) mice. Fed animals were injected intraperitoneally with 1 unit/kg body wt of human regular insulin. Blood glucose was measured immediately before injection and 15, 30, and 60 min after the injection. Results expressed as percentage of initial blood glucose concentration are means ± SEM ($n = 10–20$). *B*: Glucose tolerance tests were performed on 2-, 4-, 6-, and 12-month old control (○) and iLIRKO (●) mice that had been fasted for 16 h. Animals were injected intraperitoneally with 2 g/kg body wt of glucose. Blood glucose was measured immediately before injection and 30, 60, 90, and 120 min after the injection. Results are expressed as mean blood glucose concentration ± SEM; $n = 10–20$ of each genotype. **$P < 0.005$; *$P < 0.05$; iLIRKO versus control.

in similar growth retardation and lipoatrophy, causes diabetes without β-cell hyperplasia (23). These findings suggest that insulin regulates growth independently of metabolism and that the number of insulin receptors is an important determinant of the specificity of insulin action. In the present study, we have used an inducible strategy to generate IR deficiency in liver; thus, we obtained mice with variable levels of IR deletion (liver mosaicism). Based on this iLIRKO model, induction of liver IR deficiency after weaning caused progressive insulin resistance and glucose intolerance without alterations in liver growth. Under our experimental conditions, the effects of insulin on growth and metabolic regulation are mutually independent. Thus, deletion of liver IR in young adults gave rise to irreversible insulin resistance and progressive glucose intolerance, which persisted for up to 1 year, although liver damage was not observed in any iLIRKO mice.

Previous studies with conditional knockouts and reconstitution models concluded that the progression of insulin resistance to diabetes with fasting hyperglycemia requires defects in tissues other than liver (7,8). Moreover, acute deletion of IR in the liver has been reported to impair insulin signaling but does not induce insulin resistance or hyperinsulinemia (24). Our results in iLIRKO demonstrate that liver-specific disruption of IR can impair both hepatic and extrahepatic insulin signaling and that the severity of this resistance depends on the extent of IR deletion in the liver. iLIRKO mice display early insulin resistance as a primary defect related directly to the reduction or ablation

of liver IR, but they also have impaired insulin signaling in other peripheral tissues, including skeletal muscle and brain. Thus, iLIRKO mice present systemic insulin resistance as a secondary effect. Given that our deletion strategy did not alter IR expression in other tissues, this effect is likely the result of desensitization of the IR in extrahepatic tissues produced by prolonged hyperinsulinemia. Thus, our results demonstrate that a primary defect in the liver triggers secondary insulin resistance in extrahepatic tissues and suggest that the progression to diabetes in iLIRKO mice does not require defects other than liver IR deficiency.

Insulin resistance is associated with hyperinsulinemia and leads to β-cell hyperplasia. Thus, total deletion of liver IR induced β-cell hyperplasia in LIRKO animals (8). However, conditional inactivation of IR in muscle was not associated with either islet hyperplasia or elevated circulating levels of insulin (11). Our results with iLIRKO demonstrate a direct relationship between the level of IR expression remaining in the liver and the fold increase of plasma insulin levels and β-cell mass. Finally, constitutive LIRKO mice displayed dysregulation of insulin secretion for more than 1 year. However, in iLIRKO mice, compensatory hyperinsulinemia in 1-year-old mice was much lower than in 6-month-old mice. Thus, in our model, a failure in insulin secretion by β-cells seems to occur given the inhibition of insulin clearance in the liver, the major site where insulin is degraded in an IR-dependent manner (25). More importantly, the observations from iLIRKO
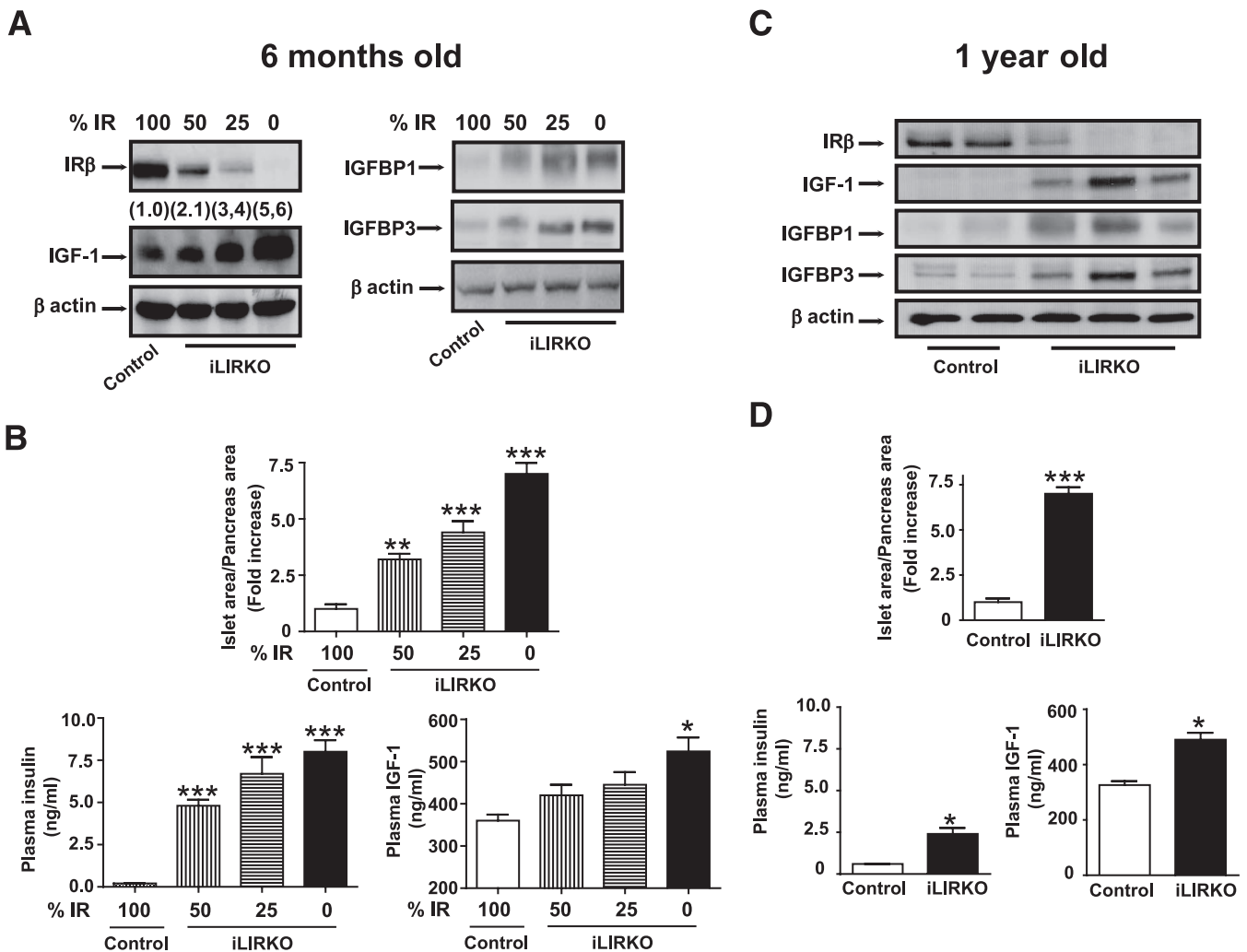
FIG. 4. Progressive IGF-1 liver expression, β-cell hyperplasia, and defective insulin secretion with aging in inducible liver-specific insulin receptor knockout (iLIRKO). *A*: Liver extracts from 6-month-old control and iLIRKO mice with graded IR deletion were analyzed by Western blot with anti-IR β-chain, IGF-1, IGFBP1, IGFBP3, and β-actin antibodies. The Western blot autoradiograms of IGF-1 were quantified by scanning densitometry from four independent experiments. *B, upper panel*: β-cell mass was evaluated by point-counting morphometry in 6-month-old control (□) and iLIRKO mice (mice with 50% IR, ▦; mice with 25% IR, ▤; mice with 0% IR, ■), results shown as fold increase of β-cell mass in control animals, *n* = 7–15 of each group. *Lower left panel*: plasma insulin content was measured in 6-month-old male control (□) and iLIRKO mice (50% IR, ▦; 25% IR, ▤; 0% IR, ■) by RIA (Linco); values are expressed as means ± SEM from four animals per genotype. *Lower right panel*: plasma IGF-1 content was measured in 6-month-old male control (□) and iLIRKO mice (50% IR, ▦; 25% IR, ▤; 0% IR, ■) by RIA (Diagnostic Systems Laboratories). Values are expressed as mean ± SEM from four animals per genotype. *C*: Liver extracts from 1-year-old control and iLIRKO mice were analyzed by Western blot with anti-IR β-chain, IGF-1, IGFBP1, IGFBP3, and β-actin antibodies. A representative experiment out of four is shown. *D, upper panel*: β-cell mass was evaluated by point-counting morphometry in 1-year-old control and iLIRKO mice; results are presented as fold increase of the control β-cell mass. *Lower left panel*: plasma insulin content was measured in 1-year-old male control and iLIRKO mice by RIA (Linco); values are expressed as means ± SEM from four animals per genotype. *Lower right panel*: plasma IGF-1 content was measured in 1-year-old male control and iLIRKO mice by RIA (Linco); values are expressed as means ± SEM from four animals per genotype. *P < 0.05, **P < 0.005, and ***P < 0.001 iLIRKO versus control.

suggest that owing to severe insulin resistance and prolonged hypersecretion of insulin, the β-cells ultimately undergo a failure to secrete insulin.

Previous evidence demonstrated that insulin signaling is essential for β-cell growth (10,26). Recently, double deficiency for IR in the liver and the β-cells was unable to induce β-cell hyperplasia in response to severe insulin resistance (27). In fact, the persistence of robust hyperplasia in 6-month-old hypoglycemic LIRKO mice supports the concept of a glucose-independent circulating islet growth factor (27). In this context, iLIRKO mice displayed increased liver IGF-1 expression dependent on the extent of IR deletion in the liver. This resulted in a persistent increase of plasma IGF-1, consistent with the fact that the liver is the main source of circulating IGF-1 (28). Previous data demonstrated that conditional deletion of IGF-1R in

the β-cell does not alter islet β-cell mass growth, suggesting a role for this receptor in regulating differentiated function (29). Surprisingly, we have found a relationship between hyperinsulinemia and β-cell hyperplasia based on an increase of genes related to β-cell proliferation and differentiation in iLIRKO mice. Thus, IGF-1 signaling might be involved in the induction of genes related to glucose-stimulated insulin secretion, among others. IGFBPs regulate the systemic effects of IGF-1 in a complex manner (30). Interestingly, IGFBP1 was upregulated in parallel to IGF-1 in iLIRKO mice, effects that were dependent on the level of hepatic IR deletion. These results are entirely consistent with the insulin-mediated effect on the IGFBP1 gene expression in liver cells (31). IGFBP1, which is mainly produced by the liver in the adult mice, inhibits IGF-dependent cellular growth in vivo (30,32,33). In addi-
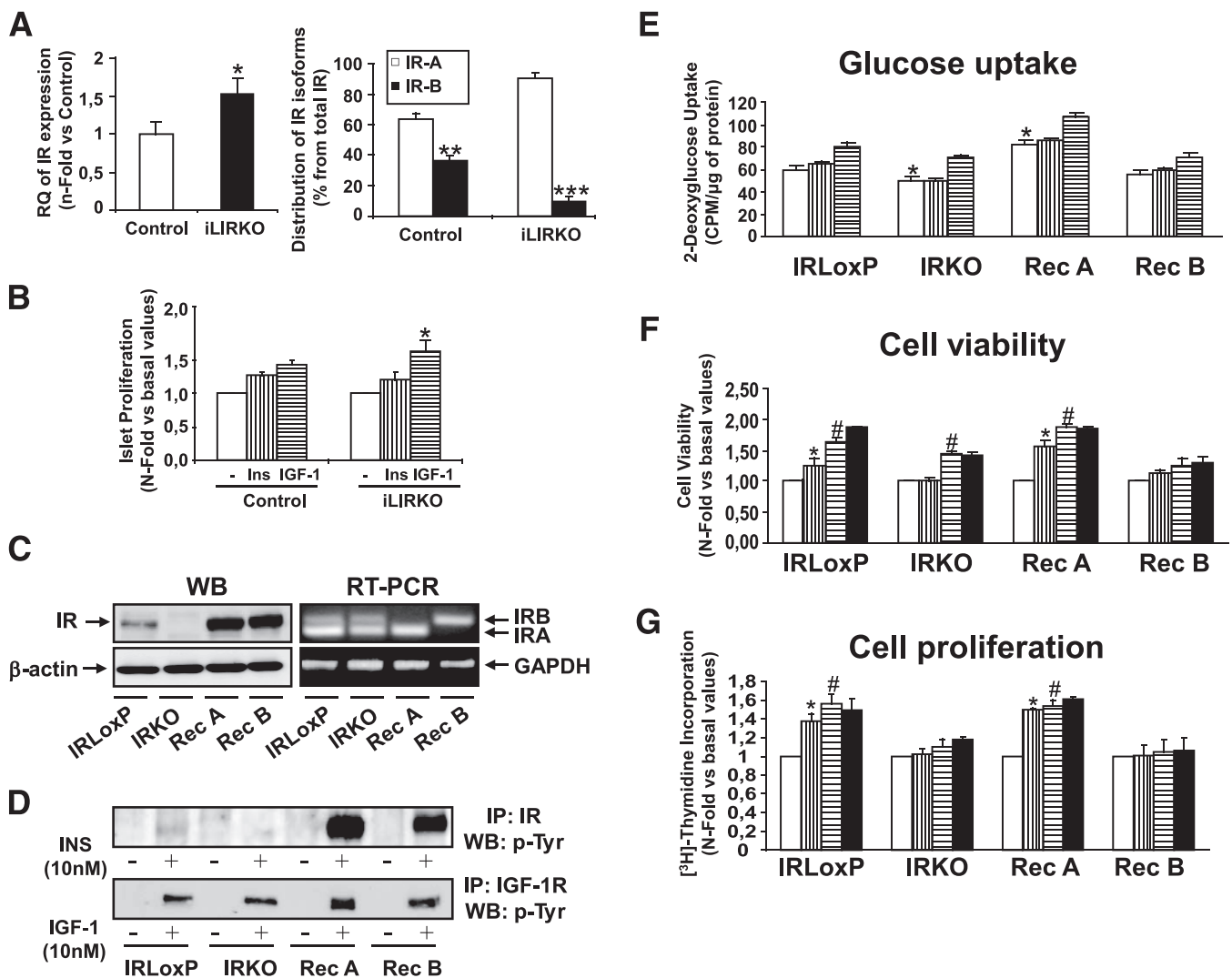
FIG. 5. Increase of IR-A isoform in pancreatic islets: β-cell lines expressing IR-A (Rec A), but not IR-B (Rec B), induce proliferation in response to insulin or IGF-1. *A:* mRNA levels of insulin receptor and the insulin receptor isoforms distribution were analyzed by real-time quantitative PCR in 6-month-old control and iLIRKO mice as described in RESEARCH DESIGN AND METHODS. Values are expressed as mean ± SEM; *n* = 4 of each genotype, (*$P < 0.05$; **$P < 0.005$; ***$P < 0.001$ iLIRKO vs. control). *B:* Pancreatic islet proliferation was assessed by BrdU incorporation in 6-month-old control and inducible liver-specific insulin receptor knockout (iLIRKO) mice. The islets were isolated as described and seeded in 96-well plates for 16 h in RPMI medium. After that, the medium was removed and fresh medium with the stimuli (10 nmol/l insulin, ▨; 10 nmol/l IGF-1, ▤) and BrdU was added for 24 h. Finally, the BrdU incorporation was measured as indicated by the manufacturer. Values are expressed as mean ± SEM; *n* = 4 of each genotype. Data were subjected to ANOVA with Bonferroni post-test (*$P < 0.05$; IGF-1 vs. basal in iLIRKO mice). *C:* IR expression was analyzed by Western blot and RT-PCR in IRLoxP, IRKO, Rec A, and Rec B β-cells. Arrow at the RT-PCR panels indicates the IR-A and IR-B. A representative experiment out of four is shown. *D:* Functional assessment of insulin receptor reconstitution was carried out by immunoprecipitation of insulin– or IGF-1–stimulated β-cells with antibodies against IR and IGF-1R and subsequent Western blot against phospho-tyrosine residues. *E:* IRLoxP, IRKO, Rec A, and Rec B β-cells were cultured to 80% confluence and then serum and glucose starved for 4–6 h. Glucose uptake induced by insulin (▨) or IGF-1 (▤) was measured as described in RESEARCH DESIGN AND METHODS. Data were subjected to ANOVA with Bonferroni post-test (*$P < 0.05$, IRKO and Rec A vs. IRLoxP in basal conditions; #$P < 0.05$, IGF-1 vs. basal of each cell line). *F:* IRLoxP, IRKO, Rec A, and Rec B β-cells were cultured to 50% confluence in 10% FBS-DMEM overnight. After that, 10 nmol/l insulin (▨), 10 nmol/l IGF-1 (▤), or both (■) were added to the wells in serum-starved 5 mmol/l glucose DMEM. After 24 h, the medium was withdrawn and the four cell lines were stained with violet crystal as described in RESEARCH DESIGN AND METHODS. Statistical significance was carried out by Student's *t* test by comparison of basal conditions with insulin-stimulated conditions of each cell line (*$P < 0.05$) or basal conditions with IGF-1–stimulated conditions of each cell line (#$P < 0.05$). *G:* IRLoxP, IRKO, Rec A, and Rec B β-cells were cultured to 50% confluence in 10% FBS-DMEM overnight. After that, 10 nmol/l insulin (▨), 10 nmol/l IGF-1 (▤), or both (■) were added to the wells in serum-starved 5 mmol/l glucose DMEM for 24 h. Thymidine incorporation was measured in these conditions as described in RESEARCH DESIGN AND METHODS. Statistical significance was carried out by Student's *t* test by comparison of basal conditions with insulin-stimulated conditions of each cell line (*$P < 0.05$) or basal conditions with IGF-1–stimulated conditions of each cell line (#$P < 0.05$).

tion, adult transgenic mice showed glucose intolerance and fasting hyperglycemia and hyperinsulinemia. However, the hyperinsulinemia observed in IGFBP1 transgenic mice cannot be attributable to insulin resistance alone (34,35). In fact, adult IGFBP1 transgenic mice displayed larger and more numerous β-cell islets reflecting increased β-cell proliferation (36). The increase of plasma IGF-1 and IGFBP1 in iLIRKO mice contrasts with IGF-1 decreases

and IGFBP1 increases in liver-specific Irs1$^{-/-}$:Irs2$^{-/-}$ mice, a mouse model also showing β-cell mass hyperplasia (37). Finally, the levels of IR were increased in the pancreatic islets of iLIRKO as compared with controls. Moreover, we noted an increase in the expression of IR-A versus IR-B in pancreatic islets from iLIRKO mice. Under our experimental conditions, IGF-1-induced proliferation was significantly higher in pancreatic islets from iLIRKO

mice than in controls. These data strongly support the notion that increased expression of IR-A relative to IR-B may enhance the growth response of pancreatic β-cell to IGF-1. Moreover, based on our observations in mouse β-cell lines, the presence of mostly IR-A in pancreatic islets may cause initially an increase in glucose uptake, a classic mitogenic signal in β-cells (17) and, subsequently, enhanced proliferation in response to either insulin or IGF-1. Alternatively, an increase in IRS-2 in pancreatic islets from iLIRKO mice may account for their enhanced proliferation in response to IGF-1. Our data obtained in pancreatic islets microarrays from iLIRKO versus control mice rule out that possibility (results not shown). Taken all together, our findings imply that IR-A, but not IR-B, confers a proliferative capacity to β-cells, which enables them to respond to insulin or IGF-1; this hypothesis may account for the β-cell hyperplasia induced by liver insulin resistance in iLIRKO mice. Thus, our results in iLIRKO mice seem to suggest a liver-pancreas endocrine axis, whereby increased plasma IGF-1 functions as a liver-derived growth factor to promote compensatory β-cell hyperplasia through IR-A.

In conclusion, our results demonstrate that hepatic IR deficiency can lead to systemic insulin resistance. Given that insulin resistance states can be compensated for by β-cell hyperplasia, studies of iLIRKO emphasize a cause-and-effect relationship between progressive insulin resistance and β-cell hyperplasia. Ultimately, the β-cells fail to secrete sufficient insulin, and this leads to uncontrolled diabetes. Thus, in iLIRKO mice, hepatic insulin resistance is sufficient to recapitulate the progressive pathogenesis of type 2 diabetes. IGF-1 expression was enhanced depending on the extent of hepatic IR deletion, and this resulted in a persistent increase of circulating IGF-1 in iLIRKO mice. Concurrently, IR-A expression was significantly increased in pancreatic islets of iLIRKO mice, presumably providing a mechanism by which the proliferative response to IGF-I was enhanced in the hyperplastic pancreatic islets of iLIRKO mice. Thus, our studies of iLIRKO mice suggest a liver-pancreas endocrine axis in which IGF-1 functions as a liver factor to promote compensatory β-cell hyperplasia through IR-A.

ACKNOWLEDGMENTS

REFERENCES

1. Kahn CR: Banting Lecture: Insulin action, diabetogenes, and the cause of type 2 diabetes. *Diabetes* 43:1066–1084, 1994
2. Kahn CR: Diabetes: causes of insulin resistance. *Nature* 373:384–385, 1995
3. Nandi A, Kitamura Y, Kahn CR, Accili D: Mouse models of insulin resistance. *Physiol Rev* 84:623–647, 2004
4. Kitamura T, Kahn CR, Accili A: Insulin receptor knockout mice. *Annu Rev Physiol* 65:313–332, 2003
5. Accili D, Drago J, Lee EJ, Johnson MD, Cool MH, Salvatore P, Asico LD, Jose PA, Taylor SI, Westphal HD: Early neonatal death in mice homozygous for a null allele of the insulin receptor gene. *Nat Genet* 12:106–109, 1996
6. Joshi RL, Lamothe B, Cordonnier N, Mesbah K, Monthioux E, Jami J, Buchini D: Targeted disruption of the insulin receptor gene in the mouse results in neonatal lethality. *EMBO J* 15:1542–1547, 1996
7. Okamoto H, Nakae J, Kitamura T, Park BC, Dragatsis I, Accili D: Transgenic rescue of insulin receptor–deficient mice. *J Clin Invest* 114:214–223, 2004
8. Michael MD, Kulkarni RN, Postic C, Previs SF, Shulman GI, Magnuson MA, Kahn CR: Loss of insulin signaling in hepatocytes leads to severe insulin resistance and progressive hepatic dysfunction. *Mol Cell* 6:87–97, 2000
9. Bruning JC, Gautam D, Burks DJ, Gillette J, Schubert M, Orban PC, Klein R, Krone W, Muller-Wieland D, Kahn CR: Role of brain insulin receptor in control of body weight and reproduction. *Science* 289:2122–2155, 2000
10. Kulkarni RN, Bruning JC, Winnay JN, Postic C, Magnuson MA, Kahn CR: Tissue-specific knockout of the insulin receptor in pancreatic β cells creates an insulin secretory defect similar to that in type 2 diabetes. *Cell* 96:329–339, 1999
11. Bruning JC, Michael MD, Winnay JN, Hayashi T, Horsch D, Accili D, Goodyear LJ, Kahn CR: A muscle-specific insulin receptor knockout exhibits features of the metabolic syndrome of NIDDM without altering glucose tolerance. *Mol Cell* 2:559–569, 1998
12. Kühn R, Schwenk F, Aguet M, Rajewsky K: Inducible gene targeting in mice. *Science* 269:1427–1429, 1995
13. Valverde AM, Lorenzo M, Pons S, White MF, Benito M: IRS-1 and IRS-2 differential signaling in the insulin/IGF-1 pathways in fetal brown adipocytes. *Mol Endocrinol* 12:688–697, 1998
14. Guerra C, Navarro P, Valverde AM, Arribas M, Bruning J, Kozak LP, Kahn CR, Benito M: Brown adipose tissue-specific insulin receptor knockout shows diabetic phenotype without insulin resistance. *J Clin Invest* 108:1205–1213, 2001
15. Weibel ER: *Practical Research Design and Research Design and Methods for Biological Morphometry.* London, Academic Press, 1979
16. Bonner-Weir S, Deery D, Leahy JL, Weir GC: Compensatory growth of pancreatic beta-cells in adult rats after short-term glucose infusion. *Diabetes* 38:49–53, 1989
17. Guillen C, Navarro P, Robledo M, Valverde AM, Benito M: Differential mitogenic signaling in insulin receptor-deficient fetal pancreatic beta-cells. *Endocrinology* 147:1959–1968, 2006
18. Nevado C, Benito M, Valverde AM: Role of insulin receptor and balance in insulin receptor isoforms A and B in regulation of apoptosis in simian virus 40-immortalized neonatal hepatocytes. *Mol Cell Biol* 19:1185–1198, 2008
19. Escribano O, Arribas M, Valverde AM, Benito M: IRS-3 mediates insulin-induced glucose uptake in differentiated IRS-2(-/-) brown adipocytes. *Mol Cell Endocrinol* 30:1–9, 2007
20. Escribano O, Fernández-Moreno MD, Zueco JA, Menor C, Fueyo J, Ropero RM, Diaz-Laviada I, Román ID, Guijarro LG: Insulin receptor substrate-4 signaling in quiescent rat hepatocytes and in regenerating rat liver. *Hepatology* 37:1461–1469, 2003
21. Flier SN, Kulkarni RN, Kahn CR: Evidence for a circulating islet cell growth factor in insulin-resistant status. *Proc Natl Acad Sci U S A* 98:7475–7480, 2001
22. McClain DA: Different ligand affinities of the two human insulin receptor splice variants are reflected in parallel changes in sensitivity for insulin action. *Mol Endocrinol* 5:734–739, 1991
23. Kitamura T, Kitamura Y, Nakae J, Giordano A, Cinti S, Kahn CR, Efstratiadis A, Accili D: Mosaic analysis of insulin receptor function. *J Clin Invest* 113:209–219, 2004
24. Buettner C, Patel R, Muse ED, Bhanot S, Monia BP, McKay R, Obici S, Rossetti L: Severe impairment in liver insulin signaling fails to alter hepatic insulin action in conscious mice. *J Clin Invest* 115:1306–1313, 2005
25. Duckworth WC, Bennett RG, Hamel FG: Insulin degradation: progress and potential. *Endocr Rev* 19:608–624, 1998
26. Withers DJ, Gutierrez JS, Towery H, Burks DJ, Ren JM, Previs S, Zhang Y, Bernal D, Pons S, Shulman GI, Bonner-Weir S, White MF: Disruption of IRS-2 causes type 2 diabetes in mice. *Nature* 391:900–904, 1998
27. Okada T, Liew CW, Hu J, Hinault C, Michael MD, Krutzfeld J, Yin C, Holzember M, Stoffel M, Kulkarni RN: Insulin receptors in beta-cells are critical for islet compensatory growth response to insulin resistance. *Proc Natl Acad Sci U S A* 104:8977–8982, 2007
28. Yakar S, Rosen CJ, Beamer WG, Ackert-Bicknell CL, Wu Y, Liu JL, Ooi GT, Setser J, Frystyk J, Boisclair YR, Leroith D: Circulating levels of IGF-1 directly regulate bone growth and density. *J Clin Invest* 110:771–781, 2002

29. Kulkarni RN, Holzenberger M, Shih DQ, Ozcan U, Stoffel M, Magnuson MA, Kahn CR: β-Cell–specific deletion of the Igf1 receptor leads to hyperinsulinemia and glucose intolerance but does not alter β-cell mass. *Nat Genet* 31:111–115, 2002

30. Schneider MR, Lahm H, Wu M, Hoeflich A, Wolf E: Transgenic mouse models for studying the functions of insulin-like growth factor-binding proteins. *FASEB J* 14:629–640, 2000

31. Guo S, Rena G, Cichy S, He X, Cohen P, Unterman T: Phosphorylation of serine 256 by protein kinase B disrupts transactivation by FKHR and mediates effects of insulin on insulin-like growth factor-binding protein-1 promoter activity through a conserved insulin response sequence. *J Biol Chem* 274:17184–17192, 1999

32. Gay E, Seurin D, Babajko S, Doublier S, Cazillis M, Binoux M: Liver-specific expression of human insulin-like growth factor binding protein-1 in transgenic mice: repercussions on reproduction, ante- and perinatal mortality and postnatal growth. *Endocrinology* 138:2937–2947, 1997

33. Rajkumar K, Barron D, Lewitt MS, Murphy LJ: Growth retardation and hyperglycemia in insulin like growth factor binding protein-1 transgenic mice. *Endocrinology* 136:4029–4034, 1995

34. Rajkumar K, Dheen ST, Murphy LJ: Hyperglycemia and impaired glucose tolerance in insulin-like growth factor binding protein-1 transgenic mice. *Am J Physiol* 270:E565–E571, 1996

35. Rajkumar K, Krsek M, Dheen ST, Murphy LJ: Impaired glucose homeostasis in insulin-like growth factor binding protein-1 transgenic mice. *J Clin Invest* 98:1818–1825, 1996

36. Dheen ST, Rajkumar K, Murphy LJ: Islet cell proliferation and apoptosis in insulin-like growth factor binding protein-1 in transgenic mice. *J Endocrinol* 155:551–558, 1997

37. Dong XC, Copps KD, Guo S, Li Y, Kollipara R, DePinho RA, White MF: Inactivation of hepatic foxo1 by insulin signaling is required for adaptive nutrient homeostasis and endocrine growth regulation. *Cell Metab* 8:65–76, 2008